Modeling of vascular interactions in endochondral ossification using human embryonic stem cells-derived organoid on a microfluidic chip

Abhiraj Kesharwani[1], Shoichiro Tani[2], Masaki Nishikawa[3], Yasuyuki Sakai[3], Hiroyuki Okada[2,4], Shinsuke Ohba[5], Ung-il Chung[1,2], Hironori Hojo[1,2,*]

[1]Department of Bioengineering, Graduate School of Engineering, The University of Tokyo, Tokyo 113-8654, Japan.
[2]Center for Disease Biology and Integrative Medicine, Graduate School of Medicine, The University of Tokyo, Tokyo 113-8654, Japan.
[3]Department of Chemical Systems Engineering, Graduate School of Engineering, The University of Tokyo, Tokyo 113-8654, Japan.
[4]Department of Orthopaedic Surgery, Graduate School of Medicine, The University of Tokyo, Tokyo 113-8654, Japan.
[5]Department of Tissue and Developmental Biology, Graduate School of Dentistry, Osaka University, Osaka 565-0871, Japan.
*Corresponding author: hojo@g.ecc.u-tokyo.ac.jp (H.H.)

Highlights

- Vascular-like structures are constructed by the microfluidic chip platform.
- The SH organoid is developed by mixing hESC-derived sclerotome and HUVECs.
- The SH organoid-on-a-chip shows the vascular-like networks.

Keywords

Endochondral ossification, Vascular interaction, Human embryonic stem cells, Sclerotome cells, Microfluidic platform, Organoid-on-a-chip

Abbreviations

HUVECs, human umbilical vein endothelial cells; Scl, Sclerotome; SH, sclerotome and HUVECs; VEGF, vascular endothelial growth factor; ECM, extracellular matrix

Abstract

Vascular interactions play a crucial role in skeletal development. In endochondral ossification, a mode of skeletal development, vascular invasion into the cartilage mold triggers ossification. We and other groups developed a model of endochondral ossification by implanting human embryonic stem cell (hESC)-derived sclerotomes into immunodeficient mice. However, in vitro models of endochondral ossification, particularly at the vascular interaction stage, are yet to be established. Therefore, we developed a model of the vascular interactions using an organoid method and a microfluidic chip-based platform. The organoids consisted of hESC-derived sclerotomes and human umbilical vein endothelial cells (HUVECs) and were named SH organoids. On the chip, we found that the fibrin gel helped align mCherry-labeled HUVECs better than the collagen-I gel, suggesting a better vascular network-like structure. The perfusability of the vascular-like structure was partially observed using fluorescein isothiocyanate (FITC)-dextran and fluorescent microbeads. The SH organoids maintained better integrity in the mCherry-labeled vascular-like network than the sclerotome spheroids. The EGFP-positive HUVECs migrated from the SH organoid, formed a vascular-like structure, and partially interacted with the mCherry-labeled vascular-like networks in the chip. Given that sclerotome gives rise to skeletal cell types, this study demonstrates that the SH organoid-on-a-chip model can recapitulate vascular interactions that may be involved in endochondral ossification. This model may provide insights into human endochondral ossification and has potential applications in bone disease modeling and drug screening.

1. Introduction

Bone creates the framework of the human body, maintains mineral concentrations, and provides niches for hematopoietic cells. Bone is a highly vascularized tissue, and the vascular network is crucial for bone development, growth, metabolism, and healing. Embryonic skeletal development occurs via two distinct processes: endochondral and intramembranous ossification. Intramembranous ossification gives rise to typical flat bones, mainly in the calvaria, and involves the direct differentiation of osteoblast precursors into bone-forming osteoblasts. Conversely, the development of most bones, including the long bones, proceeds via endochondral ossification. During endochondral ossification, mesenchymal cells condense to form a cartilage template. Within this template, the chondrocytes proliferate and differentiate into hypertrophic chondrocytes. These hypertrophic chondrocytes secrete growth factors, including bone morphogenetic protein (BMP), hedgehog, and vascular endothelial growth factor (VEGF). VEGF plays an important role in facilitating vascular interactions with the avascular cartilage tissue, where neighboring blood vessels penetrate the cartilage. This process leads to the replacement of cartilage with bone, contributing to the formation of the bone marrow structure[1–3].

Although basic knowledge of bone development has been accumulated, mainly in animal models, the mechanisms underlying human bone development are not fully understood. Thus, recapitulating endochondral ossification using human embryonic stem cell (hESC) is highly desired [4–6]. We recently studied gene regulatory mechanisms in bone development using an hESCs model in which hESC-derived sclerotome cells were implanted underneath the renal capsule of immunodeficient mice [7]. We observed that the induced sclerotome self-assembled to form the bone tissue. However, this system requires an *in vivo* mouse environment, in which blood vessels are

constructed using mouse cells in the induced bone. To develop a fully human model, an *in vitro* system that recapitulates human blood-vessel invasion is required.

The recently developed organoid method and organ-on-a-chip technology have enabled recapitulation of *in vivo* development more precisely. An organoid is a self-organized 3D tissue consisting of multiple cells derived from hESCs or other cells [8–9]. This technology provides a valuable platform for modeling human organ development and investigating various diseases [10]. An organ-on-a-chip is a system engineered using microfluidic technology, where microfluidic chips are designed to recapitulate the 3D microstructures of tissues [11–13]. These technologies have been used to model several organs, including bone marrow. However, the modeling of endochondral ossification, specifically vascular interactions, has not yet been reported. Because sequential bone development involves multiple cell types, recapitulating this step is challenging in an *in vitro* system.

In this study, we aimed to model vascular interactions using an organoid model with hESCs-derived sclerotome and the organ-on-a-chip technology. We optimized a commercially available microfluidic-based chip device and developed an organoid model that enables the formation of vascular interactions between blood vessel-like tissues.

2. Methods

2.1 Human embryonic stem cell culture and maintenance

We conducted experiments involving hESCs, adhering to the Ministry of Health guidelines and obtaining Ethics Committee approval from the University of Tokyo (#19-203). As previously described, we used the SEES3 hESC line [14]. The initial adaptation and maintenance of hESCs were carried out in a commercially available xenofree culture system, utilizing StemFit AK02N medium (#AK02N, Ajinomoto), and dishes were coated with 5 ug/mL recombinant human vitronectin (#A14700, Gibco). The cells were cultured under optimal conditions at 37 °C with 5% CO_2 in a humid environment. For efficient cell dissociation, 0.5 M EDTA (#15575-020, Gibco) was meticulously diluted to 0.5 mM using Dulbecco's Phosphate-Buffered Saline (DPBS) (#049-29793, Wako). To ensure enhanced cell viability during seeding or passaging, 10 μM Y-27632 (#034-24024, Fujifilm Wako) was used to prevent apoptosis.

2.2 Sclerotome differentiation of hESC under xenofree conditions

Subconfluent, undifferentiated hESCs were gently dissociated into small clumps by approximately 10 rounds of pipetting. These cells were then sparsely passaged at a ratio of 1:16 to 1:24 depending on the size of the hESC colonies. The passaging was performed onto new vitronectin-coated culture plates using StemFit AK02N medium supplemented with 1 μM Y-27632 overnight. It is crucial to sparsely seed the hESCs before differentiation to minimize the risk of cellular overgrowth, particularly during prolonged differentiation periods. Differentiation into sclerotomes was systematically conducted in a serum-free, xeno-free, feeder-free monolayer environment using a chemically defined B27/ITS medium (BIM) [7]. The BIM was prepared and sclerotome induction was performed following a previously established methodology [7]. In brief, BIM was prepared by combining 1% B27 Supplement Xeno-Free (#A1486701, Thermo Fisher Scientific), 1% ITS Liquid Media Supplement (#I3146, Sigma-Aldrich), 1% MEM Non-Essential Amino Acids Solution (#11140050, Thermo Fisher Scientific), and 55 μM 2-

Mercaptoethanol (0.1% of 55 mM 2-Mercaptoethanol in DPBS) (#21985023, Thermo Fisher Scientific) in Dulbecco's Modified Eagle Medium/Nutrient Mixture F-12 (DMEM/F12) (#11330032, Thermo Fisher Scientific). The hESCs were differentiated into sclerotomes (Scls) using a stepwise protocol (Fig. S1A): induction from hESCs to primitive streak by treatment with 5 μM CHIR99021 (#4423, Tocris); induction from primitive streak to paraxial mesoderm by treatments with 5 μM CHIR99021, 1 μM A 83-01 (#2939, Tocris), and 0.25 μM LDN193189 (#SML0559; Sigma); induction from paraxial mesoderm to somitic mesoderm by treatments with 1 μM C59 (#C7641-2S; Cellagen Technology), 1 μM A 83-01, and 0.25 μM LDN193189; induction from somitic mesoderm to sclerotome by treatments with 1 μM SAG (#AG-CR1-3585, Adipogen), 1 μM C59, and 0.25 μM LDN193189. All inductions were performed for 24 h, except for sclerotome induction, which lasted for 48 h.

2.3 Construction of a lentivirus vector

The pLenti-mCherry-Puro vector was constructed using the HiFi assembly kit (#E2621S, NEB) with an mCherry-T2A-PuroR (puromycin resistant gene) fragment into a lentiviral vector. The backbone of the lentiviral vector was prepared by removing the mCherry fragment from the pLV-mCherry vector (Plasmid #36084, Addgene).

2.4 Lentivirus preparation

HEK293T cells (#CRL-3216, ATCC) were cultured in Dulbecco's Modified Eagle's medium (DMEM), supplemented with 10% fetal bovine serum and 1% penicillin/streptomycin (#P4333, Sigma-Aldrich). The maintenance of cells occurred in a tissue culture incubator at 37 °C with 5% CO2. Upon reaching 60-70% confluency, HEK293T cell transfection was carried out using FuGENE® HD (#E2312, Promega) and Opti-MEM (#31985-070, Thermofisher) following the manufacturer's instructions. Plasmids for VEGFA-EGFP lentivirus production included pCCLc-MNDU3-VEGFA-PGK-EGFP-WPRE (Plasmid #89609, Addgene), pMD2.G (Plasmid #12259, Addgene), and psPAX2 (Plasmid #12260, Addgene). For mCherry lentivirus production, the pmCherry-puromycin vector, pMD2.G, and psPAX2 were used. The FuGENE HD reagent and Opti-MEM were incubated for 30 min at room temperature. For a single 10 cm dish, a mixture was prepared comprising 8.5 μg of pCCLc-MNDU3-VEGFA-PGK-EGFP-WPRE for VEGFA-EGFP transfection, or alternatively, 8.5 μg of pmCherry-Puro for mCherry transfection, along with 2.1 μg of pMD2.G, and 6.4 μg of psPAX2. The volume was adjusted by adding Opti-MEM to reach 799 μL, and then 51 μL of FuGENE HD transfection reagent was introduced to achieve the final volume of 850 μL. After combining the plasmids and reagent at room temperature, the mixture was added to HEK293T cells in a 100 mm dish containing 10 mL DMEM with 10% fetal bovine serum and 1% penicillin and streptomycin (#168-23191, Fujifilm Wako Pure Chemical). Following 48 hours of transfection, the cell culture medium was harvested and filtered using a 0.45 μm filter. For lentiviral storage and concentration, a Lenti-X concentrator (#631231, Takara) was used according to the manufacturer's protocol. A concentrated lentivirus suspension was used to transduce the HUVECs.

2.5 HUVECs lentiviral transduction

HUVECs (#00191027 XL size, Lonza) were cultured in Endothelial Growth Medium 2 (EGM2) (#CC-3162, Lonza) and maintained in a tissue culture incubator at 37 °C with 5% CO_2. Lentiviral transduction was conducted

the following day when HUVECs reached an optimal confluency range of 40–50%. A concentration of 6 μg/mL Polybrene (#107689-10G, Sigma) was included in the lentiviral transduction process. After 48–72 h of transduction, GFP expression from VEGFA-EGFP lentivirus transduction or RFP expression from mCherry lentivirus transduction was observed under a fluorescence microscope. Overexpression of VEGFA was validated using RT-qPCR.

2.6 SH organoid formation with SH (Sclerotome Spheroid + HUVECs) method-

Sclerotome cells derived from hESCs and HUVECs overexpressing VEGFA were dissociated using Accutase (#AT104, Innova Cell Technologies) and a 2.5% trypsin-EDTA solution (#T4174-100mL, Wako), respectively. After counting, centrifuging, and collecting the cells, sclerotome cells and HUVECs were resuspended in SCL induction medium with 1 μM Y-27632 and EGM2, respectively. For the formation of SH organoids, sclerotome cells and HUVECs were mixed in a 4:1 ratio in SH medium and 3×10^4 cells per well were seeded into a 96-well ultra-low attachment plate (#7007, Corning). The SH medium was prepared by combining EGM2 and the SCL induction medium with 1 μM Y-27632 in a 9:1 ratio. After the initial 24-hour incubation period, the culture medium was changed to the EGM2 medium, and subsequently, the EGM medium was changed every other day (Fig. S1A).

2.7 Mimetas OrganoPlate® Graft plate

The OrganoPlate® Graft plate (#6401-400-B, Mimetas), is a microfluidic platform comprising 64 chips, specifically designed to fit into a standard 384-well plate. Each chip contained three distinct channels: one center channel for gel loading and two peripheral channels for the culture medium. The OrganoPlate® Graft was originally intended for vascularizing tumor spheroids [15], but here we chose SH organoids to utilize the available open access (with a 1 mm diameter) and to establish the vascular-like structures underneath the gel chamber. Interaction between the SH organoid and vascular-like structures was observed under a fluorescence microscope.

2.8 Gel loading, and Microvascular network formation-

For gel loading, fibrinogen (#F3879-100MG, Sigma) and thrombin (#T6884-100UN, Sigma) stock solutions were prepared at concentrations of 15 and 100 U/mL, respectively, in DPBS. Then fibrin solution was prepared by combining 300 μL of 15 mg/mL fibrinogen with 10 μL of 100 U/mL thrombin in DPBS, resulting in a final volume of 1000 μL. The final working concentrations of thrombin and fibrinogen in the fibrin solution were 1 U/mL, and 4.5 mg/mL respectively. Subsequently, 3 μL of the fibrin solution were immediately injected onto the inlet of the gel chamber following the addition of thrombin to the fibrinogen solution. It was visually confirmed that the fibrin solution completely filled the gel chambers. Next the OrganoPlate® Graft was incubated at 37 °C for 15 min to facilitate fibrin gel crosslinking. To prevent the drying of the fibrin gel, 50 μL of Hanks' balanced salt solution (HBSS) (#H8264-100ML, Sigma) was added to the gel inlet.

To initiate the formation of microvascular networks, mCherry-expressing HUVECs were dissociated using a 2.5% trypsin-EDTA solution. After counting, centrifuging, and collecting the mCherry-expressing HUVECs, 2 μL of the cell suspension, with each microliter containing 10,000 cells, were added to each perfusion channel. Subsequently, 50 μL of EGM2 was introduced into each perfusion inlet, and the plate was incubated at

37 °C with 5% CO_2 for 2–4 h under stable conditions. After the attachment of cells in the perfusion channels, an additional 50 µL of EGM2 was applied to each perfusion outlet to establish complete medium flow within the perfusion channels. Then the HBSS was aspirated from the gel inlet, and 50 µL of EGM2 was introduced into the graft chamber. Following this, the plate was cultured for 2-3 days on a rocking stage (OrganoFlow, Mimetas, USA) with a 14° inclination and an 8-minute interval to allow bidirectional flow in the chip. These specific culture conditions were maintained to promote the formation of tube-like structures within the perfusion channels, in accordance with the recommendations of Mimetas for optimal vessel formation and maintenance. Subsequently, the device underwent stimulation with 50 µL of an angiogenic cocktail, comprising rhVEGF-165 (#100-20, Peprotech) (37.5 ng/mL), rhFGFb (#100-18B, Peprotech) (37 ng/mL), rhHGF (#11343413, ImmunoTools) (37.5 µg/mL), rhMCP-1 (#11343384, ImmunoTools) (37.5 ng/mL), PMA (#P1585, Sigma) (37.5 ng/mL), and S1P (#S9666, Sigma) (250 nM), aiming to induce the formation of a vascular-like structures in the graft chamber. The angiogenic cocktail was changed every day, the EGM2 in the perfusion channels was changed every 2 days, and the culture was continued on a rocker for 3-4 days for microvascular formation.

2.9 SH organoid grafting in the chip

On day 14, an SH organoid within the size range of 500 to 700 µm was carefully chosen from the organoid culture maintained under EGM2 conditions. Using a 200 µL-sized tip, the organoid was picked up and grafted into the chip's graft chamber where a microvascular bed was present. The positioning of the organoid was fine-tuned using a needle to ensure its placement in the central part of the chamber. Following organoid grafting, 50 µL of an angiogenic cocktail was introduced into the graft chamber, and this cocktail was replaced daily and EGM2 in perfusion channels were changed on alternate days throughout the 7-day culture period in the chip.

2.10 Sprout perfusability

To assess the perfusability of the constructed vascular bed within the chip, we introduced a solution of fluorescent microbeads (#T7284, TetraSpeck™ Fluorescent Microspheres Sampler Kit, ThermoFisher) and 70 kDa FITC-dextran (#53471-1G, Sigma) on day 7 into both perfusion inlets following removal of the cultured EGM2 medium. The fluorescent microbead solution comprised beads sized at 4 µm, each possessing four distinct excitation/emission peaks: 360/430 nm (blue), 505/515 nm (green), 560/580 nm (orange), and 660/680 nm (dark red), with a concentration ranging from 7×10 ^5 to 14×10 ^5 beads per milliliter in PBS. The green fluorescent microbeads were visualized for several minutes using a BZ-X700 fluorescence microscope (Keyence).

FITC-dextran solution was prepared by dissolving 0.5 mg 70 kDa FITC-dextran (0.5 mg) in 1 mL of the EGM2 medium. This solution was added both peripheral channels of the chip and observations were performed for several minutes using a BZ-X700 fluorescence microscope.

2.11 Gel area and sprouting quantification

The gel area was quantified using Fiji (ImageJ), whereas the evaluation of sprouting involved tallying the number of vessels and measuring their lengths using the same software. The length of each vessel was determined by tracing from the edges of the perfusion channels (on both sides) to the endpoint within the extracellular matrix

(ECM). To quantify the vascular area, only the vascular-like networks within the gel were analyzed and expressed as a percentage.

3. Results

3.1 Establishing a microvascular-like network in a microfluidic chip.

To mimic the formation and interactions of peripheral blood vessels surrounding cartilage tissue during endochondral ossification, we aimed to establish microvascular networks within a microfluidic chip system. We utilized the OrganoPlate® Graft from Mimetas, a versatile multichip microfluidic platform containing 64 individual chips per plate (Fig. 1a). Each chip featured two main peripheral channels connecting wells A1 to B1 and A3 to B3 along with a gel chamber with a gel-loading inlet in well A2 and open access in well B2. The organoid can be positioned in the open-access gel in well B2 (Fig. 1a, 1b). The process of forming a vascular-like network is as follows: extracellular matrix (ECM) and endothelial cells are introduced through the gel inlet and both peripheral channels, respectively. After tube formation, angiogenic factors can be added to well B2 to induce sprouting from the peripheral channels. Following the establishment of a vascular-like network, the organoid can be introduced, allowing the observation of vascular interactions with the organoid (Fig. 1b).

To optimize the culture conditions for forming vascular networks in the chip, we evaluated two extracellular matrix (ECM) materials: collagen-I gel and fibrin gel. Both gels were prepared and loaded into the gel inlet of the chip. Following gel crosslinking, mCherry-expressing HUVECs were cultured in both perfusion channels of the chip for 2–3 days (Fig. 2A). Subsequently, an angiogenic cocktail containing VEGFA, FGF-2, MCP-1, HGF, S1P, and PMA was added to promote the formation of vascular network structures within the graft chamber (Fig. 2B). Morphological assessments showed that although both matrices exhibited minimal shrinkage prior to exposure to the angiogenic cocktail, the collagen-I gel shrank considerably compared to the fibrin gel (Fig. 2C). This caused detachment of the gel from the peripheral channels, resulting in no contact between peripheral channels and vascular-like networks. In contrast, the fibrin gel formed vascular-like structures in the presence of the angiogenic cocktail without significant shrinkage and keeping the contact between peripheral channels and vascular-like networks. The number of vessels generated, and their lengths were significantly higher in the fibrin gel than in the collagen-I gel from days 4 to 7 (Fig. 2D). Additionally, vessel lengths were significantly increased in the fibrin gel compared to the collagen-I gel on days 6 and 7 (Fig. 2D).

Perfusability tests were conducted on the vascular bed within the fibrin gel. We introduced 70 kDa FITC-dextran into both perfusion channels. We found that perfusion began immediately after the introduction of FITC-dextran into the perfusion channels. At 0 s, FITC-dextran showed perfusion through the vascular bed and reached the center of the graft chamber during long-term observation until 240 s (Fig. 2E). For further confirmation, a 4 μm size-fluorescent bead suspension was introduced into the perfusion inlets at 0 s (Supplementary Video 1). After 156 s, we observed fluorescent beads traversing the vascular-like networks within the chip (Supplementary Video 2). Hence, our findings indicate that fibrin gel exhibits superior qualities to collagen-I gel in the chip environment for aligning HUVECs, possibly providing better vascular-like networks in the chip.

3.2 Sclerotome spheroid and SH organoid on the perfusable vascular-like network.

To effectively mimic vascular interactions with skeletal cells, we hypothesized that organoid formation by mixing sclerotomes, osteochondral progenitors, and HUVECs would help form vascular-like networks in the chip. Using a previously published method for sclerotome induction, we optimized organoid formation (Fig. S1A). We set day 0 as the day of organoid formation (Fig. S1B). We also confirmed that sclerotome cells on day 0 showed downregulated expression of the pluripotency marker genes *NANOG* and *POU5F1* and upregulated expression of the sclerotome marker genes *PAX1* and *PAX9* (Fig. S1B). To enhance visibility of HUVECs, we labeled the cells with EGFP and used these cells for the SH (Sclerotome and HUVECs) organoid formation. We used two distinct 3D models, sclerotome spheroids and an engineered SH organoid from hESC-derived sclerotomes mixed with EGFP-expressing HUVECs (Fig. S1B). Once the vascular-like network fully developed within the graft chamber, the sclerotome spheroids and SH organoids were introduced into the graft chamber of the chip. We used the angiogenic cocktail for one week of sclerotome spheroid and SH organoid cultures to maintain a vascular-like network in the chip. During culture, we observed connections between mCherry-expressing HUVECs from peripheral channels and EGFP-expressing HUVECs from the SH organoid, suggesting the formation of vascular-like tissue. (Fig. 3A). By day 14, the integrity of the vascular-like structure was compromised to some extent under both chip conditions. To assess vascular integrity, we examined mCherry-expressing vascular-like network areas on days 8 (Fig. 3B, C) and 14 (Fig. 3D, E). Microscopic images and quantitative analysis showed comparable vascular-like networks under both conditions on day 8 (Fig. 3B, C). On day 14, although we observed degradation of the vascular-like networks under both conditions, the integrity of the vascular-like network was higher in the SH organoid-on-a-chip than in the sclerotome spheroid-on-a-chip (Fig. 3D, E). These results indicate that the SH organoid-on-a-chip maintained significantly better vascular integrity than the sclerotome spheroid-on-a-chip throughout the 14-day culture period.

To assess the interaction between the SH organoid and the peripheral vascular-like network, we observed fluorescent microscopic images of the SH organoid-on-a-chip. We found that the SH organoids formed EGFP-expressing vascular-like structures within the matrix on day 8 in the chip, characterized by the emergence of small GFP-expressing vascular-like sprouts extending from the SH organoids (Fig. 4A). The vascular-like sprouts extended and reached the peripheral mCherry-expressing vascular-like networks by day 10, whereas no connections were observed between the GFP- and mCherry-expressing vascular networks (Fig. 4B). Throughout the continued culture of the SH organoid in the chip, the EGFP- and mCherry-expressing vascular-like networks were connected as vascular-like structures by day 12 (Fig. 4C). 3D construction using z-stack images from day 12 of the SH organoid-on-a-chip showed vascular-like network connections between GFP- and mCherry-expressing HUVECs (Fig. 4D). In summary, these findings demonstrate that the SH organoid-on-a-chip maintained the integrity of the vascular-like network better than the sclerotome spheroid-on-a-chip. Because sclerotome gives rise to skeletal cells, this SH organoid can partially replicate vascular interactions during endochondral ossification in vitro using a microfluidic chip platform.

4. Discussion

This study had three major findings. First, the fibrin gel formed better vascular-like networks than the collagen-I

gel on the chip. Second, the SH organoid can form a vascular-like network in the organoid and interact with the peripheral vascular-like networks. Third, the SH organoid-on-a-chip maintained the integrity of the vascular-like structure better than the sclerotome spheroid. Collectively, we developed the SH organoid-on-a-chip system that allows 3D vascular-like network interactions in the chip.

The ECM plays a crucial role in vascular networks, and fibrin gel is better than collagen-I gel in our system. Although previous studies have used collagen-I gel for hepatic spheroids in the same organ-on-a-chip system (Organoplate® Graft) [16], we observed shrinkage of the collagen-I gel during the induction of vascular networks with an angiogenic cocktail. Consistent with our results, Jung et al. applied the same fibrin gel to the same chip system with different contents and formed a vascular network using primary human pulmonary microvascular endothelial cells, fibroblasts, and pericytes [15]. Nashimoto et al. used fibrin–collagen gel in a custom-made chip system [17] . However, maintaining the integrity of a vascular network on a chip remains challenging. As shown by Bonanini, et al., [16] we observed vascular degradation during culture. Our observations suggest that after the grafting of organoids, cells from the organoid start migrating into the matrix and quickly cover the ECM during culture. This has a negative impact on the vascular network integrity. However, this phenomenon was not controlled in this system [18]. Therefore, to maintain vascular integrity, it is important to inhibit the migration of cells from organoids. Additional studies are needed to develop a better system or ECM to prevent cell migration from the organoid tissue.

In this study, we developed the SH organoid: mixing hESC-derived sclerotome and HUVECs. This method helps the formation of vascular-like structure within the organoid. In addition, in the SH organoid on a chip system, vascular-like networks were observed between vascular-like structure from the SH organoid and that from the surrounding area in a 3D environment. This was inspired by other studies suggesting that using pre-vascularized organoids can improve the vascularization in the organoid as well as supporting vascular integration with the peripheral vascular networks on a chip. In addition, the use of a pre-vascularized organoid can increase the possibility of on-a-chip anastomosis [16–17–19]. We successfully created similar vascular-like network interactions using SH organoid-on-a-chip system. However, three limitations of this study must be overcome. First, vascular interactions with cartilage tissue are necessary for endochondral ossification. In this study, we used hESCs-derived sclerotome that includes skeletal progenitors; however, those cells have not been differentiated into mature skeletal cells yet. Given that hypertrophic chondrocytes secrete angiogenic factors for vascular interactions, maturation of the SH organoid is the next challenge. Second, the perfusion of vascular networks in organoids must be developed. Although we confirmed the perfusion of the vascular networks formed by peripheral channels, perfusion into the organoid has not yet been achieved. One possible solution may be to develop a chip device that ensures close contact of organoids with surrounding vascular networks, as demonstrated by Quintard et al. [19]. Additionally, as confirmed by Nashimoto et al., increasing the size of the pores in the peripheral channels can induce wider vascular networks (>100 μm diameter), which can enhance the interaction and possibly invade the organoid-on-a-chip [17]. Finally, although our study demonstrates the successful formation of a vascular-like network and on-a-chip interactions, there remains a gap in the long-term culture of SH organoids on-a-chip. As previous studies using the same chip system had limited culture periods for different cell types [16–18], we believe that the development of a chip system is required. Recently, several circulatory systems have been developed for long-term organoid culture

[19]. Thus, these systems are promising for long-term culture applications.

5. Conclusions

Our model partially demonstrates a proof-of-concept of the vascular interaction stage in endochondral ossification. Although further improvements are required, this concept may contribute to a better understanding of human bone development and diseases, potentially paving the way for the discovery of novel therapeutic targets in the future.

Acknowledgments

We thank Sakurako Hayashi, Dahlia Eldeeb, Shant Nepal, Priscillia Christiany, Ireen James, Jinyan Si, Maki Kurihara, Dr. Shinse Fujita, Chie Kataoka, Asuka Uchida, and Nozomi Nagumo at The University of Tokyo for providing technical assistance. This work was supported by Grants-in-Aid for Scientific Research from the Japan Society for the Promotion of Science (JSPS: 21H04952), Rising Star Award from American Society for Bone and Mineral Research, the Japan Science and Technology Agency FOREST Program (JPMJFR225N). This work utilized the core research facility of the Center for Disease Biology and Integrative Medicine at The University of Tokyo Graduate School of Medicine. A.K. was supported by the Japan International Cooperation Agency (JICA) Friendship programs.

Figures/Figure legends

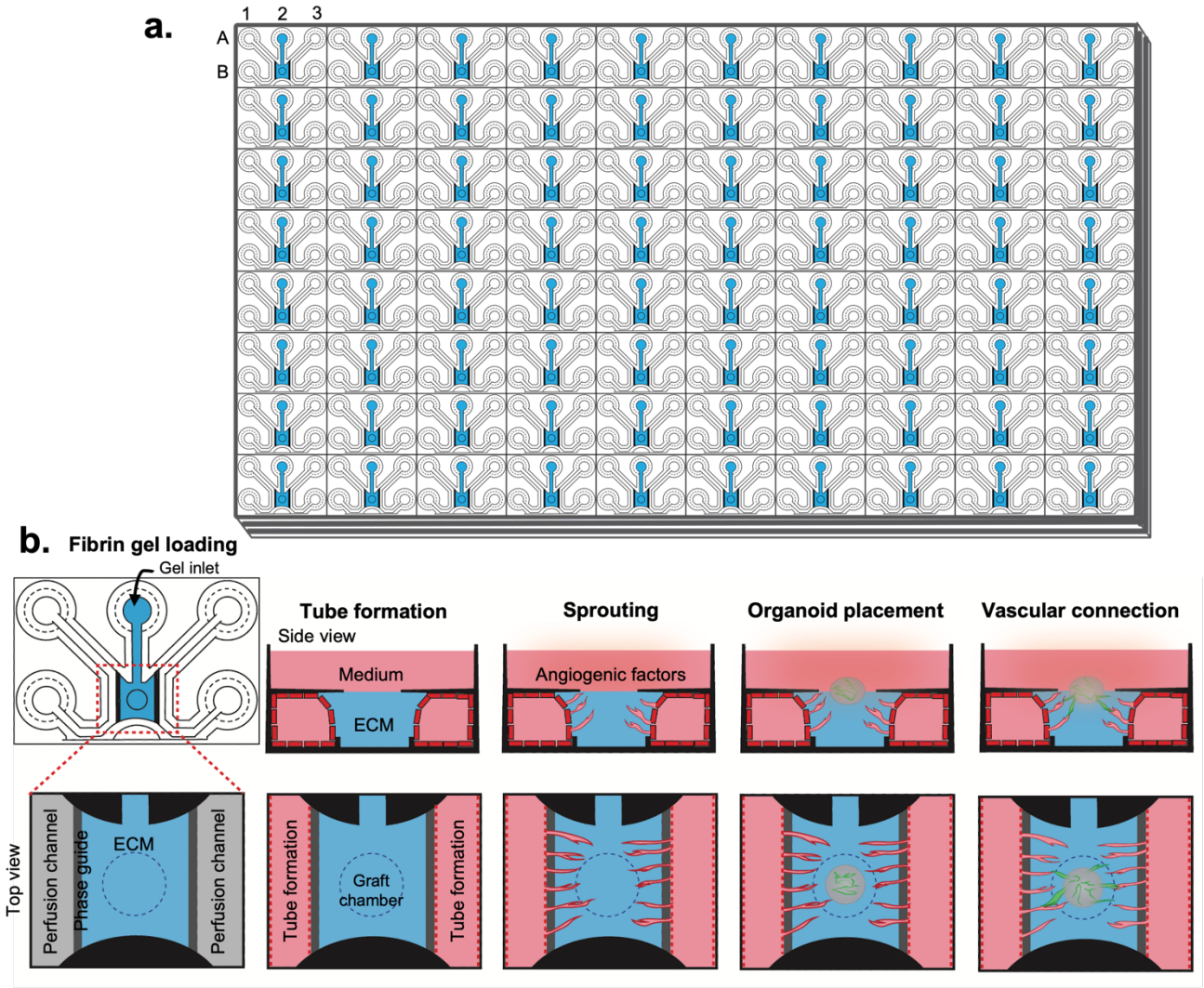

Fig.1. Schematic of human cartilage organoid-on-a-chip.

(a) Illustration of the Mimetas OrganoPlate® Graft, consisting of 384 wells and 64 chips. (b) Illustration of experimental steps for the blood vessels interaction into the organoid. Fibrin gel loading: the gel is loaded through the gel inlet. Tube formation: HUVECs are seeded in the perfusion inlets and vessel tube formation under flow. Sprouting: vascular network is formed using an angiogenic cocktail. Organoid placement: organoid is placed in a graft chamber. Vascular connections: vascular connection occurs between the organoid and vascular from peripheral channel.

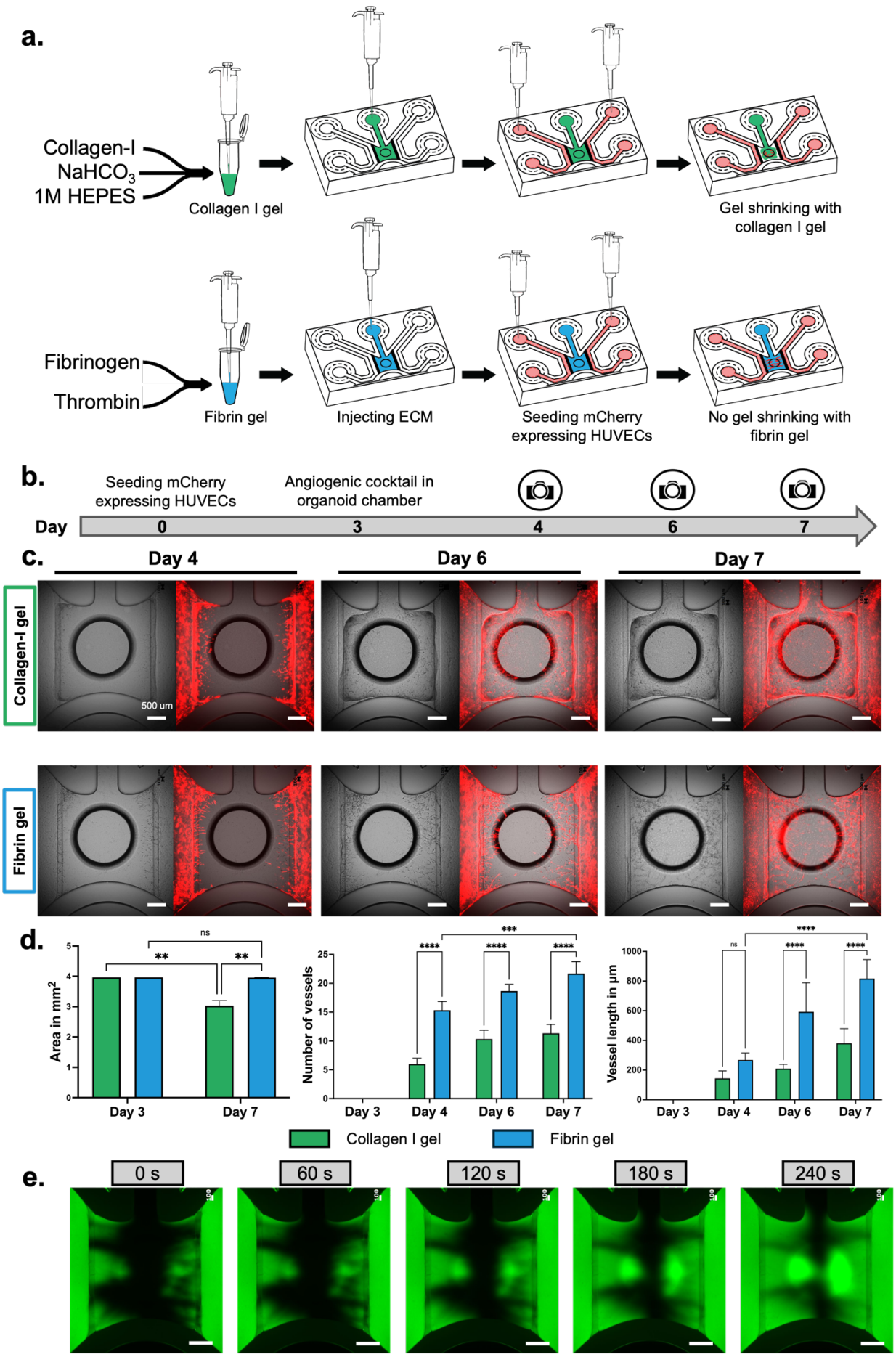
a.
Collagen-I
NaHCO3
1M HEPES
Collagen I gel
Gel shrinking with collagen I gel
Fibrinogen
Thrombin
Fibrin gel
Injecting ECM
Seeding mCherry expressing HUVECs
No gel shrinking with fibrin gel
b.
Seeding mCherry expressing HUVECs
Angiogenic cocktail in organoid chamber
Day
0
3
4
6
7
c.
Day 4
Day 6
Day 7
Collagen-I gel
Fibrin gel
500 um
d.
Area in mm²
Number of vessels
Vessel length in µm
Day 3
Day 4
Day 6
Day 7
Collagen I gel
Fibrin gel
e.
0 s
60 s
120 s
180 s
240 s

Fig.2. Development of perfusable microvascular networks.

(a) Representation of vascular bed formation with collagen-I and fibrin gel loading and HUVECs seeding in perfusing inlets. (b) Timeline for vascular bed formation. (c) Bright field and merged images represent the angiogenesis using collegen-I gel and fibrin gel. Scale bar: 500 μm. (d) Comparative analysis between collagen-I gel and fibrin gel in terms of gel area, number of vessels formed, and vessel length over seven days of microvascular network formation. A two-way ANOVA with multiple comparisons was used to analyze the data. Statistical significance is indicated by ** for $p < 0.01$, *** for $p < 0.001$, and **** for $p < 0.0001$. (e) Validation of vascular bed perfusibility in fibrin gel using 70 kDa FITC-dextran represented as a green fluorescent fluid for long-term observation. Scale bar: 500 μm.

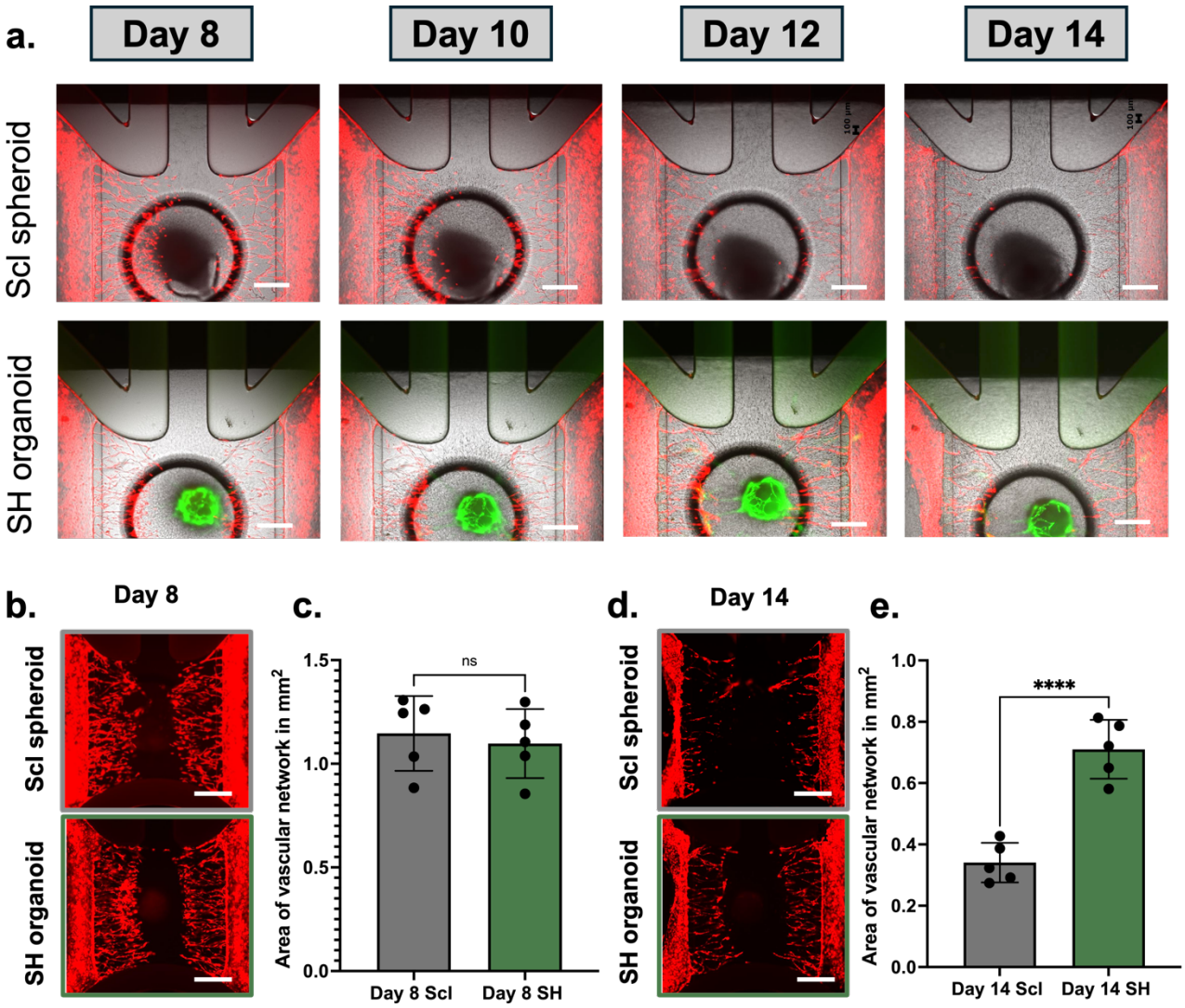

Fig.3. Sclerotome spheroid and SH organoid culture on a microvascular network.

(a) Fluorescent microscopic images of sclerotome spheroid- and SH organoid-on-a-chip captured from day 8 to day 14. (b, c) Fluorescent image of mCherry expressing vascular networks (b) and the quantification analysis (c) on day 8 for sclerotome spheroid- and SH organoid-on-a-chip. (d, e) Fluorescent image of mCherry expressing vascular networks (d) and the quantification analysis (e) on day 14 for sclerotome spheroid- and SH organoid-on-a-chip. In A, B, D, Scale bar: 500 µm. In c, e, Scl, sclerotome spheroid; SH, SH organoid. For statistical analysis Student's t-test was used, "*" indicates statistical significance (****$p < 0.0001$) and "ns" represents not significant.

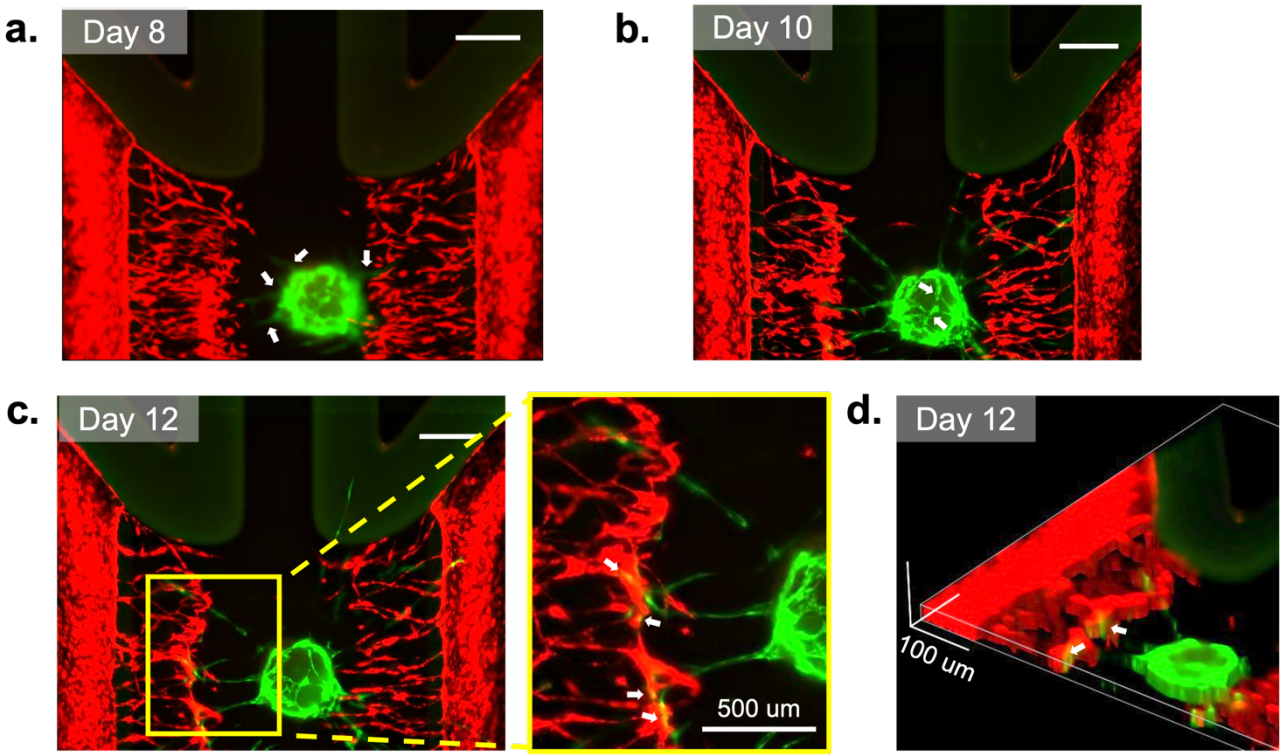

Fig.4. Interaction between SH organoid and peripheral vascular network by mCherry positive HUVECs from peripheral channels and EGFP positive HUVECs from the SH organoid.

(a) Fluorescent microscopy images showing vascular networks on day 8 (a), day 10 (b) and day 12 (c). White arrows show the vascular networks. In (c), yellow box is zoomed up on the right side. (d) 3D reconstruction of the vascular network images using FIJI. White arrows show the vascular networks interactions. For (a), (b), (c) scale bar: 500 µm.

Supplementary data

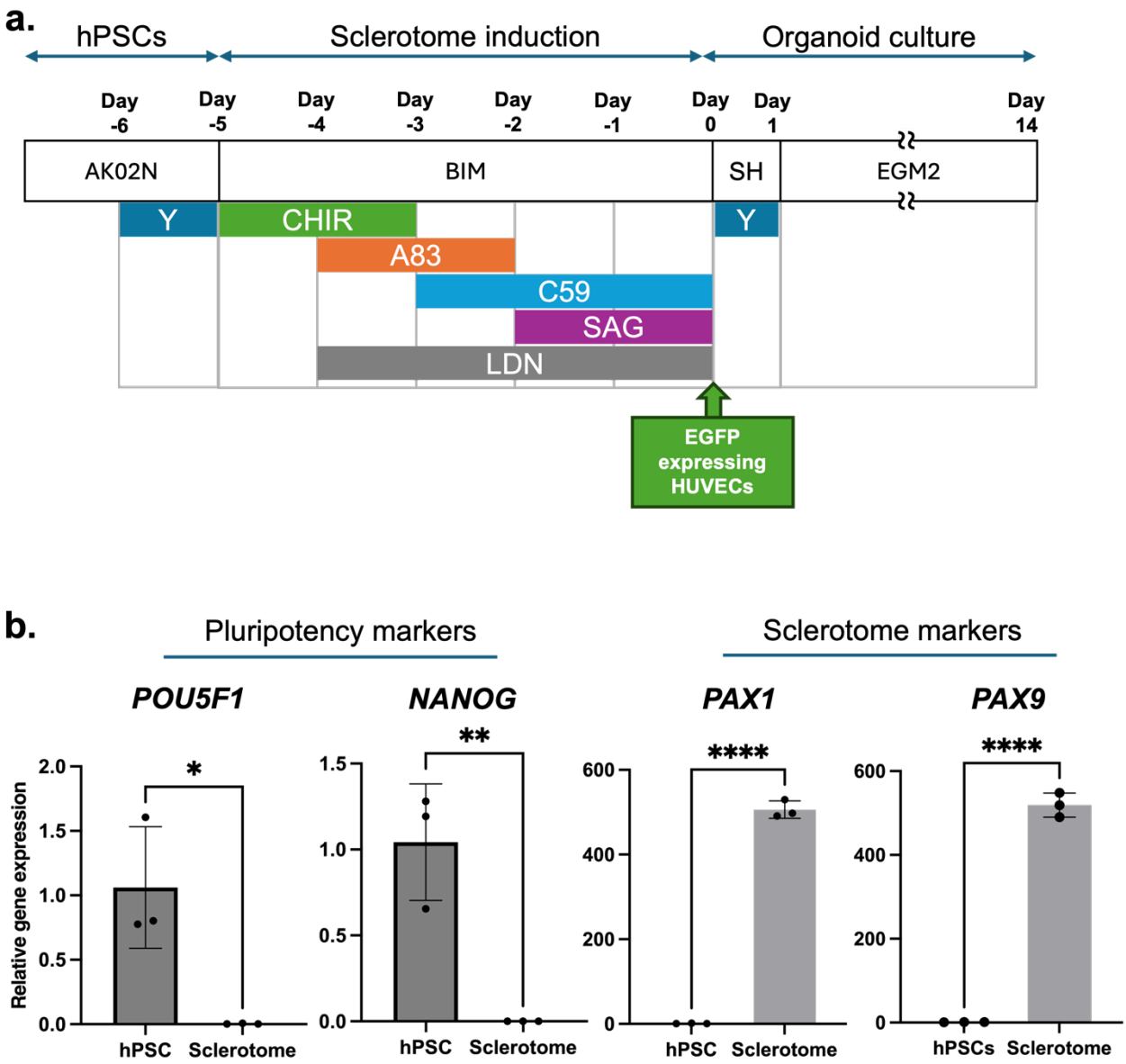

Fig. S1. Experimental scheme of the sclerotome induction and organoid culture. (a) Sclerotome spheroids are induced form hESCs-derived sclerotome cells using different small molecules, but SH organoid is the mixture of sclerotome and EGFP expressing HUVECs. (b) Relative gene expression of pluripotent markers on day -6 and sclerotome markers on day 0, determined by RT-qPCR. Student's t-test was used to analyze the data, "*" indicates statistical significance (*$p < 0.05$; **$p < 0.01$; ****$p < 0.0001$).

Reference:

1. B. R. Olsen, A. M. Reginato, & W. Wang, *BONE DEVELOPMENT* (2000).
2. K. J. Rambhia & P. X. Ma, Biomineralization and Bone Regeneration DEVELOPMENT AND FRACTURE OF BONE Bone Development. *Principles of Regenerative Medicine*, (2019).

3. A. Teti, Bone development: Overview of bone cells and signaling. *Current Osteoporosis Reports*, **9** (2011). https://doi.org/10.1007/s11914-011-0078-8.
4. Y. Pretemer, S. Kawai, S. Nagata, M. Nishio, M. Watanabe, S. Tamaki, C. Alev, Y. Yamanaka, J. Y. Xue, Z. Wang, K. Fukiage, M. Tsukanaka, T. Futami, S. Ikegawa, & J. Toguchida, Differentiation of Hypertrophic Chondrocytes from Human iPSCs for the In Vitro Modeling of Chondrodysplasias. *Stem Cell Reports*, **16** (2021). https://doi.org/10.1016/j.stemcr.2021.01.014.
5. T. Kamakura, Y. Jin, M. Nishio, S. Nagata, M. Fukuda, L. Sun, S. Kawai, & J. Toguchida, Collagen X Is Dispensable for Hypertrophic Differentiation and Endochondral Ossification of Human iPSC-Derived Chondrocytes. *JBMR Plus*, **7** (2023). https://doi.org/10.1002/jbm4.10737.
6. S. R. Lamandé, E. S. Ng, T. L. Cameron, L. H. W. Kung, L. Sampurno, L. Rowley, J. Lilianty, Y. N. Patria, T. Stenta, E. Hanssen, K. M. Bell, R. Saxena, K. S. Stok, E. G. Stanley, A. G. Elefanty, & J. F. Bateman, Modeling human skeletal development using human pluripotent stem cells. *Proceedings of the National Academy of Sciences of the United States of America*, **120** (2023). https://doi.org/10.1073/pnas.2211510120.
7. S. Tani, H. Okada, S. Onodera, R. Chijimatsu, M. Seki, Y. Suzuki, X. Xin, D. W. Rowe, T. Saito, S. Tanaka, U. il Chung, S. Ohba, & H. Hojo, Stem cell-based modeling and single-cell multiomics reveal gene-regulatory mechanisms underlying human skeletal development. *Cell Reports*, **42** (2023). https://doi.org/10.1016/j.celrep.2023.112276.
8. Z. Zhao, X. Chen, A. M. Dowbaj, A. Sljukic, K. Bratlie, L. Lin, E. L. S. Fong, G. M. Balachander, Z. Chen, A. Soragni, M. Huch, Y. A. Zeng, Q. Wang, & H. Yu, Organoids. *Nature Reviews Methods Primers*, **2** (2022). https://doi.org/10.1038/s43586-022-00174-y.
9. M. Hofer & M. P. Lutolf, Engineering organoids. *Nature Reviews Materials*, **6** (2021). https://doi.org/10.1038/s41578-021-00279-y.
10. M. A. Lancaster & J. A. Knoblich, Organogenesisin a dish: Modeling development and disease using organoid technologies. *Science*, **345** (2014). https://doi.org/10.1126/science.1247125.
11. C. M. Leung, P. de Haan, K. Ronaldson-Bouchard, G. A. Kim, J. Ko, H. S. Rho, Z. Chen, P. Habibovic, N. L. Jeon, S. Takayama, M. L. Shuler, G. Vunjak-Novakovic, O. Frey, E. Verpoorte, & Y. C. Toh, A guide to the organ-on-a-chip. *Nature Reviews Methods Primers*, **2** (2022). https://doi.org/10.1038/s43586-022-00118-6.
12. Q. Wu, J. Liu, X. Wang, L. Feng, J. Wu, X. Zhu, W. Wen, & X. Gong, Organ-on-a-chip: Recent breakthroughs and future prospects. *BioMedical Engineering Online*, **19** (2020). https://doi.org/10.1186/s12938-020-0752-0.
13. A. Aazmi, H. Zhou, Y. Li, M. Yu, X. Xu, Y. Wu, L. Ma, B. Zhang, & H. Yang, Engineered Vasculature for Organ-on-a-Chip Systems. *Engineering*, **9** (2022). https://doi.org/10.1016/j.eng.2021.06.020.
14. H. Akutsu, M. Machida, S. Kanzaki, T. Sugawara, T. Ohkura, N. Nakamura, M. Yamazaki-Inoue, T. Miura, M. C. Vemuri, M. S. Rao, K. Miyado, & A. Umezawa, Xenogeneic-free defined conditions for derivation and expansion of human embryonic stem cells with mesenchymal stem cells. *Regenerative Therapy*, **1** (2015). https://doi.org/10.1016/j.reth.2014.12.004.

15. O. Jung, Y. T. Tung, E. Sim, Y. C. Chen, E. Lee, M. Ferrer, & M. J. Song, Development of human-derived, three-dimensional respiratory epithelial tissue constructs with perfusable microvasculature on a high-throughput microfluidics screening platform. *Biofabrication*, **14** (2022). https://doi.org/10.1088/1758-5090/ac32a5.
16. F. Bonanini, D. Kurek, S. Previdi, A. Nicolas, D. Hendriks, S. de Ruiter, M. Meyer, M. Clapés Cabrer, R. Dinkelberg, S. B. García, B. Kramer, T. Olivier, H. Hu, C. López-Iglesias, F. Schavemaker, E. Walinga, D. Dutta, K. Queiroz, K. Domansky, B. Ronden, J. Joore, H. L. Lanz, P. J. Peters, S. J. Trietsch, H. Clevers, & P. Vulto, In vitro grafting of hepatic spheroids and organoids on a microfluidic vascular bed. *Angiogenesis*, **25** (2022). https://doi.org/10.1007/s10456-022-09842-9.
17. Y. Nashimoto, T. Hayashi, I. Kunita, A. Nakamasu, Y. S. Torisawa, M. Nakayama, H. Takigawa-Imamura, H. Kotera, K. Nishiyama, T. Miura, & R. Yokokawa, Integrating perfusable vascular networks with a three-dimensional tissue in a microfluidic device. *Integrative Biology (United Kingdom)*, **9** (2017) 506–518. https://doi.org/10.1039/c7ib00024c.
18. T. Russell, Q. Dirar, Y. Li, C. Chiang, D. T. Laskowitz, & Y. Yun, Cortical spheroid on perfusable microvascular network in a microfluidic device. *PLoS ONE*, **18** (2023). https://doi.org/10.1371/journal.pone.0288025.
19. C. Quintard, E. Tubbs, G. Jonsson, J. Jiao, J. Wang, N. Werschler, C. Laporte, A. Pitaval, T. S. Bah, G. Pomeranz, C. Bissardon, J. Kaal, A. Leopoldi, D. A. Long, P. Blandin, J. L. Achard, C. Battail, A. Hagelkruys, F. Navarro, Y. Fouillet, J. M. Penninger, & X. Gidrol, A microfluidic platform integrating functional vascularized organoids-on-chip. *Nature Communications*, **15** (2024). https://doi.org/10.1038/s41467-024-45710-4.
20. S. El-Chemaly, G. Pacheco-Rodriguez, D. Malide, V. Meza-Carmen, J. Kato, Y. Cui, P. I. Padilla, A. Samidurai, B. R. Gochuico, & J. Moss, Nuclear localization of vascular endothelial growth factor-D and regulation of c-Myc-dependent transcripts in human lung fibroblasts. *American Journal of Respiratory Cell and Molecular Biology*, **51** (2014). https://doi.org/10.1165/rcmb.2013-0417OC.
21. V. Mariotti, R. Fiorotto, M. Cadamuro, L. Fabris, & M. Strazzabosco, New insights on the role of vascular endothelial growth factor in biliary pathophysiology. *JHEP Reports*, **3** (2021). https://doi.org/10.1016/j.jhepr.2021.100251.